Inorg. Chem. **2005**, *44*, 3422–3430

An Asymmetric Dizinc Phosphodiesterase Model with Phenolate and Carboxylate Bridges

Jingwen Chen,[†,‡] Xiaoyong Wang,[†] Yangguang Zhu,[†] Jun Lin,[†] Xiaoliang Yang,[†] Yizhi Li,[†] Yi Lu,[§] and Zijian Guo*[,†]

State Key Laboratory of Coordination Chemistry, Coordination Chemistry Institute, Nanjing University, Nanjing 210093, People's Republic of China, Yancheng Institute of Technology, Yancheng 214003, People's Republic of China, and Department of Chemistry, University of Illinois, Urbana, Illinois 61801

Received September 25, 2004

A phosphodiesterase model with two zinc centers has been synthesized and characterized. The compound, $[Zn_2(L_{-2H})(AcO)(H_2O)](PF_6)\cdot 2H_2O$ (Zn_2L'), was formed using an "end-off" type compartmental ligand, 2,6-bis{[(2-pyridylmethyl)(2-hydroxyethyl)amino]methyl}-4-methylphenol (L), and zinc acetate dihydrate. The X-ray crystallographic analysis shows that Zn_2L' contains a μ-acetato-μ-cresolato-dizinc(II) core comprised of a quasi-trigonal bipyramidal Zn and a distorted octahedral Zn, and the distance between them is 3.421 Å which is close to the dizinc distance in related natural metalloenzymes. Phosphodiesterase activity of Zn_2L' was investigated using bis(4-nitrophenyl) phosphate (BNPP) as the substrate. The pH dependence of the BNPP cleavage in aqueous buffer media shows a sigmoid-shaped pH–k_{obs} profile with an inflection point around pH 7.13 which is close to the first pK_a value of 7.20 for Zn_2L' obtained from the potentiometric titration. The catalytic rate constant (k_{cat}) is 4.60×10^{-6} s^{-1} at pH 7.20 and 50 °C which is ca. 10^5-fold higher than that of the uncatalyzed reaction. The deprotonated alcoholic group appended on Zn_2L' is responsible for the cleavage reaction. The possible mechanism for the BNPP cleavage promoted by Zn_2L' is proposed on the basis of kinetic and spectral analysis. The dizinc complex formed in situ in anhydrous DMSO exhibits a similar ability to cleave BNPP. This study provides a less common example for the phosphodiesterase model in which the metal-bound alkoxide is the nucleophile.

1. Introduction

The phosphodiesters that form the structural backbone of nucleic acids are extremely stable. It is estimated that the half-life for the hydrolysis of the phosphodiester bonds in RNA at 25 °C in water is 110 years and in DNA is on the order of billions of years.[1] However, nature has selected a variety of enzymes to efficiently catalyze the hydrolysis of nucleic acids under physiological conditions.[2] Most of these enzymes contain metal ions, typically Zn(II), Mg(II), and Fe(III), in their active centers.[2d,3] The metal centers are normally bridged by carboxyls which can bring the two metals into proximity and promote the formation of additional bridging hydroxide (or water) groups and substrate molecules.[4] For example, many natural phosphoesterases contain two or three zinc ions bridged by a carboxyl group from an aspartate residue and a water molecule in their catalytic sites (Chart 1).[2b,3c,5] These zinc enzymes often use external water molecules or internal alcoholic hydroxyl residues as nucleophiles to react with electrophilic substrates.[6]

* To whom correspondence should be addressed. E-mail: zguo@nju.edu.cn. Phone: +86 25 83594549. Fax: +86 25 83314502.
† Nanjing University.
‡ Yancheng Institute of Technology.
§ University of Illinois.

(1) (a) Westheimer, F. H. *Science* **1987**, *235*, 1173−1178. (b) Williams, N. H.; Takasaki, B.; Wall, M.; Chin, J. *Acc. Chem. Res.* **1999**, *32*, 485−493.
(2) (a) Sträter, N.; Lipscomb, W. N.; Klabunde, T.; Krebs, B. *Angew. Chem., Int. Ed. Engl.* **1996**, *35*, 2024−2055. (b) Wilcox, D. E. *Chem. Rev.* **1996**, *96*, 2435−2458. (c) Cowan, J. A. *Chem. Rev.* **1998**, *98*, 1067−1088. (d) Jedrzejas, M. J.; Setlow, P. *Chem. Rev.* **2001**, *101*, 608−618.
(3) (a) Lowther, W. T.; Matthews, B. W. *Chem. Rev.* **2002**, *102*, 4581−4607. (b) Holz, R. C. *Coord. Chem. Rev.* **2002**, *232*, 5−26. (c) Parkin, G. *Chem. Rev.* **2004**, *104*, 699−767 and references therein.
(4) He, C.; Lippard, S. J. *J. Am. Chem. Soc.* **2000**, *122*, 184−185.
(5) (a) Lipscomb, W. N.; Sträter, N. *Chem. Rev.* **1996**, *96*, 2375−2433. (b) Takagi, Y.; Warashina, M.; Stec, W. J.; Yoshinari, K.; Taira, K. *Nucleic Acids Res.* **2001**, *29*, 1815−1834. (c) Horton, N. C.; Perona, J. J. *Nat. Struct. Biol.* **2001**, *8*, 290.

10.1021/ic048654m CCC: $30.25
Published on Web 04/13/2005

Chart 1. Some Phosphoesterases that Feature a Bridging Carboxyl Unit

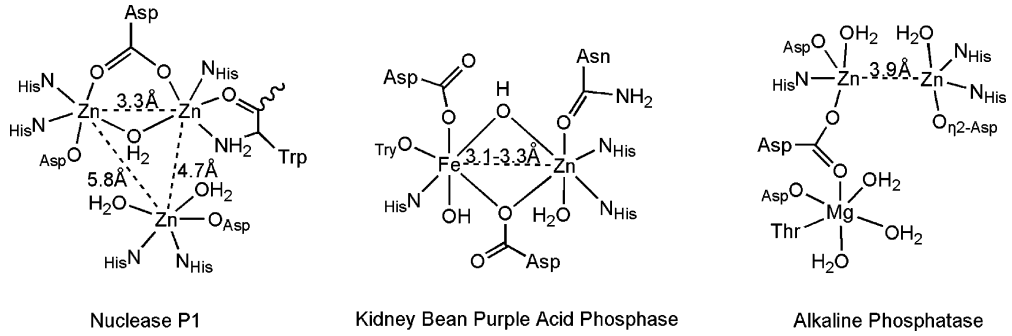

The role of zinc centers in these enzymes is to orient and activate the substrates.[2a,b,5a]

Functional mimics of phosphoesterases are important for understanding the role of metal ions in the hydrolytic mechanisms[7] and for developing artificial nucleases for biochemical and medicinal applications.[7a,b,8] Multinuclear transition metal complexes are of particular interest,[3c,9] and the divalent zinc ion is the preferred metal ion for hydrolase models because it is a strong Lewis acid with rapid ligand exchange, redox inactivity, and admittedly physiological relevancy.[3c,7a,10] Over the years, Zn(II) complexes have been studied extensively in the context of the hydrolysis of nucleic acid backbones or phosphate ester models,[4,11] and some dinuclear zinc complexes derived from phenol-based ligands have shown promising activity.[3c]

Synthetic ligands containing phenolate, carboxylate, phthalazine, and pyrazolyl have been employed to facilitate the bridging of metal ions.[3c,9h] Among them, the phenolate and carboxylate are outstanding bridging groups. Phenolate-based "end-off" compartmental ligands possess two pendant chelating arms attached to the ortho positions of the phenolic hydroxyl group. This specific structure can facilitate the formation of dinuclear metal complexes bridged by endogenous phenolic oxygen and the introduction of one or two desired exogenous carboxylates or waters.[12] A number of dinuclear complexes derived from such ligands have been introduced as the structural models for the bimetallic biosites of nuclease,[9c] phosphatase,[13] phospholipase C,[14] and other enzymes.[12a,15] Because of the bridging function of these endo- and exogenous groups, the two metal ions are brought into proximity as in most natural metalloenzmyes.[3]

Numerous simple metal hydroxides have been studied as phosphoesterase models;[16] however, less attention has been paid to metal alkoxides.[17,26b,38b] Synthesis and comparison

(6) Kim, E. E.; Wyckoff, H. W. *J. Mol. Biol.* **1991**, *218*, 449−464.
(7) (a) Hegg, E. L.; Burstyn, J. N. *Coord. Chem. Rev.* **1998**, *173*, 133−165. (b) Krämer, R. *Coord. Chem. Rev.* **1999**, *182*, 243−261. (c) Molenveld, P.; Engbersen, J. F. J.; Reinhoudt, D. N. *Chem. Soc. Rev.* **2000**, *29*, 75−86.
(8) Franklin, S. J. *Curr. Opin. Chem. Biol.* **2001**, *5*, 201−208.
(9) (a) Jurek, P. E.; Jurek, A. M.; Martell, A. E. *Inorg. Chem.* **2000**, *39*, 1016−1020. (b) Roigk, A.; Schneider, H.-J. *Eur. J. Org. Chem.* **2001**, 205−209. (c) Branum, M. E.; Tipton, A. K.; Zhu, S. R.; Que, L., Jr. *J. Am. Chem. Soc.* **2001**, *123*, 1898−1904. (d) Xia, J.; Xu, Y.; Li, S.-A.; Sun, W.-Y.; Yu, K.-B.; Tang, W.-X. *Inorg. Chem.* **2001**, *40*, 2394−2401. (e) Barros, A. M.; Lippard, S. J. *Inorg. Chem.* **2001**, *40*, 1060−1064. (f) Iranzo, O.; Elmer, T.; Richard, J. P.; Morrow, J. R. *Inorg. Chem.* **2003**, *42*, 7737−7746. (g) Zhu, L.; dos Santos, O.; Koo, C. W.; Rybstein, M.; Pape, L.; Canary, J. W. *Inorg. Chem.* **2003**, *42*, 7912−7920. (h) Bauer-Siebenlist, B.; Meyer, F.; Farkas, E.; Vidovic, D.; Cuesta-Seijo, J. A.; Herbst-Irmer, R.; Pritzkow, H. *Inorg. Chem.* **2004**, *43*, 4189−4202. (i) Gavrilova, A. L.; Bosnich, B. *Chem. Rev.* **2004**, *104*, 349−383.
(10) Coleman, J. E. *Curr. Opin. Chem. Biol.* **1998**, *2*, 222−234.
(11) (a) Yamada, K.; Takahashi, Y.; Yamamura, H.; Araki, S.; Saito, K.; Kawai, M. *Chem. Commun.* **2000**, 1315−1316. (b) Kawahara, S.-I.; Uchimaru, T. *Eur. J. Inorg. Chem.* **2001**, 2437−2442. (c) Albedyhl, S.; Schnieders, D.; Jancsó, A.; Gadja, T.; Krebs, B. *Eur. J. Inorg. Chem.* **2002**, 1400−1409. (d) Worm, K.; Chu, F.; Matsumoto, K.; Best, M. D.; Lynch, V.; Anslyn, E. V. *Chem.*−*Eur. J.* **2003**, *9*, 741−747. (e) Bonfá, L.; Gatos, M.; Mancin, F.; Tecilla, P.; Tonellato, U. *Inorg. Chem.* **2003**, *42*, 3943−3949. (f) Arca, M.; Bencini, A.; Berni, E.; Caltagirone, C.; Devillanova, F. A.; Isaia, F.; Garau, A.; Giorgi, C.; Lippolis, V.; Perra, A.; Tei, L.; Valtancoli, B. *Inorg. Chem.* **2003**, *42*, 6929−6939.
(12) (a) Suzuki, M.; Furutachi, H.; Ohkawa, H. *Coord. Chem. Rev.* **2000**, *200*−*202*, 105−129. (b) Berti, E.; Caneschi, A.; Daiguebonne, C.; Dapporto, P.; Formica, M.; Fusi, V.; Giorgi, L.; Guerri, A.; Micheloni, M.; Paoli, P.; Pontellini, R.; Rossi, P. *Inorg. Chem.* **2003**, *42*, 348−357.
(13) (a) Ghiladi, M.; McKenzie, C. J.; Meier, A.; Powell, A. K.; Ulstrup, J.; Wocadlo, S. *J. Chem. Soc., Dalton Trans.* **1997**, 4011−4018. (b) Albedyhl, S.; Averbuch-Pouchot, M. T.; Belle, C.; Krebs, B.; Pierre, J. L.; Saint-Aman, E.; Torelli, S. *Eur. J. Inorg. Chem.* **2001**, 1457−1464. (c) Abe, K.-J.; Izumi, J.; Ohba, M.; Yokoyama, T.; Okawa, H. *Bull. Chem. Soc. Jpn.* **2001**, *74*, 85−95. (d) Belle, C.; Gautier-Luneau, I.; Karmazin, L.; Pierre, J. L.; Albedyhl, S.; Krebs, B.; Bonin, M. *Eur. J. Inorg. Chem.* **2002**, 3087−3090. (e) Lanznaster, M.; Neves, A.; Bortoluzzi, A. J.; Szpoganicz, B.; Schwingel, E. *Inorg. Chem.* **2002**, *41*, 5641−5643. (f) Machinaga, H.; Matsufuji, K.; Ohba, M.; Kodera, M.; Okawa, H. *Chem. Lett.* **2002**, 716−717.
(14) Uhlenbrock, S.; Krebs, B. *Angew. Chem., Int. Ed. Engl.* **1992**, *31*, 1647−1648.
(15) Erxleben, A.; Hermann, J. *J. Chem. Soc., Dalton Trans.* **2000**, 569−575.
(16) (a) Chin, J.; Banaszczyk, M.; Jubian, V.; Zou, X. *J. Am. Chem. Soc.* **1989**, *111*, 186−190. (b) Chin, J. *Acc. Chem. Res.* **1991**, *24*, 145−152. (c) Kim, J. H.; Chin, J. *J. Am. Chem. Soc.* **1992**, *114*, 9792−9795. (d) Connolly, J. A.; Banaszczyk, M.; Hynes, R. C.; Chin, J. *Inorg. Chem.* **1994**, *33*, 665−669.
(17) Bazzicalupi, C.; Bencini, A.; Berni, E.; Bianchi, A.; Fedi, V.; Fusi, V.; Giorgi, C.; Paoletti, P.; Valtancoli, B. *Inorg. Chem.* **1999**, *38*, 4115−4122.
(18) Yergey, J. A. *Int. J. Mass Spectrom. Ion Phys.* **1983**, *52*, 337.
(19) Krebs, B.; Schepers, K.; Bremer, B.; Henkel, G.; Althaus, E.; Müller-Warmuth, W.; Griesar, K.; Haase, W. *Inorg. Chem.* **1994**, *33*, 1907−1914.
(20) Ullman, F.; Brittner, K. *Chem. Ber.* **1909**, *42*, 2523−2925.
(21) Berends, H. P.; Stephan, D. W. *Inorg. Chem.* **1987**, *26*, 749−754.
(22) (a) *SMART*, version 5.625; Bruker AXS Inc.: Madison, WI, 2000. (b) *SAINT*, version 6.01; Bruker AXS Inc.: Madison, WI, 2000. (c) *SHELXTL*, version 6.10; Bruker AXS Inc.: Madison, WI, 2000. (d) *SADABS*, version 2.03; Bruker AXS Inc.: Madison, WI, 2000.
(23) The value of ϵ differs with pH. See: Koike, T.; Kimura, E. *J. Am. Chem. Soc.* **1991**, *113*, 8935−8941.
(24) Gultneh, Y.; Khan, A. R.; Blaise, D.; Chaudhry, S.; Ahvazi, B.; Marvey, B. B.; Butcher, R. J. *J. Inorg. Biochem.* **1999**, *75*, 7−18.
(25) Deacon, G. B.; Philips, R. J. *Coord. Chem. Rev.* **1980**, *23*, 227−250.
(26) (a) Kimura, E.; Nakamura, I.; Koike, T.; Shionoya, M.; Kodama, Y.; Ikeda, T.; Shirot, M. *J. Am. Chem. Soc.* **1994**, *116*, 4764−4771. (b) Kimura, E.; Kodama, Y.; Koike, T.; Shire, M. *J. Am. Chem. Soc.* **1995**, *117*, 8304−8311. (c) Iranzo, O.; Kovalevsky, A. Y.; Morrow, J. R.; Richard, J. P. *J. Am. Chem. Soc.* **2003**, *125*, 1988−1993.

Chart 2. Schematic Drawing of Ligand L and Its Asymmetric Dinuclear Complex Zn_2L

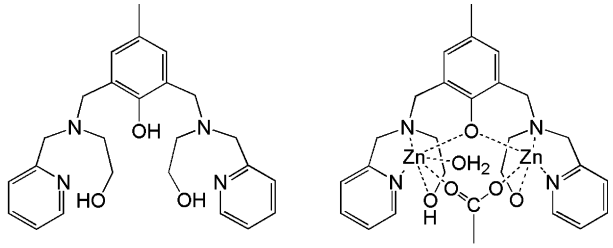

of metal alkoxide- and metal hydroxide-containing models will provide deeper insight into the structure and mechanism of phosphoesterases and help in the design of more effective metalloenzyme models. Therefore, we synthesized and characterized a novel alcoholic hydroxyl containing phenolate-based ligand L and its dinuclear zinc complex, $[Zn_2(L_{-2H})(AcO)(H_2O)]^+$ (Chart 2). The cleavage activity of the complex on the phosphate ester bond has been examined using bis(4-nitrophenyl) phosphate as the substrate (BNPP, a DNA model), and a possible cleavage mechanism is proposed on the basis of kinetic, ES-MS, and ^{31}P NMR spectral analysis.

2. Experimental Section

2.1. General Methods and Materials. The infrared spectra were recorded on a Bruker VECTOR22 spectrometer as KBr disks (4000−500 cm^{-1}). Elementary analysis was performed on a Perkin-Elmer 240C analytic instrument. Electrospray mass spectra were recorded using an LCQ electron spray mass spectrometer (ESMS, Finnigan). The isotope distribution patterns for the complex were simulated using the Isopro 3.0 program.[18] The ^1H and ^{31}P NMR spectra were recorded on a Bruker DRX-500 spectrometer at 20 and 50 °C, respectively. *J* values are in hertz. The potentiometric titration and pH measurements were carried out on a PHS-3C Exact Digital pH meter equipped with a Phonix Ag−AgCl reference electrode (Cole-Paemer Instrument Co.) which was calibrated with standard pH buffer solutions. Kinetic measurements were recorded using quartz cuvettes (1.0 cm) and a Perkin-Elmer Lambda 35 UV−vis spectrophotometer equipped with a thermostated cell compartment. Commercially available dimethyl sulfoxide (DMSO) was refluxed in the presence of CaH_2 for several hours, and then anhydrous DMSO was prepared by distilling it in vacuo over anhydrous $MgSO_4$. The buffers were prepared with *o*-phthalic acid ($pK_{a1} = 2.89$ and $pK_{a2} = 5.51$), MES (2-(*N*-morpholino)ethanesulfonic acid, $pK_a = 6.2$), and Tris (tris(hydroxymethyl)aminomethane, $pK_a = 8.3$). Other reagents and solvents were of analytical grade and used without further purification unless otherwise noted. All aqueous solutions were prepared using newly double-distilled water. Zn(II) stock solutions were titrated against EDTA following standard procedures. BNPP (sodium salt), purchased from Aldrich, was recrystallized from ethanol/water before use. Reaction solutions for BNPP cleavage were prepared according to the standard sterile techniques.

2.2. Syntheses. 2,6-Bis(2-pyridylmethyl-2-hydroxyethylamino)methyl-4-methylphenol (L). L was prepared by a method referring to the literature[19] as follows. Triethylamine (2.02 g, 20 mmol) was added to a stirred solution of 2,6-bis(chloromethyl)-4-methylphenol (BCMC) (2.05 g, 10 mmol) in absolute tetrahydrofuran (25 mL), and then the mixture was cooled to 0 °C. Then 2-pyridylmethyl-2-hydroxyethylamine (2.73 g, 20 mmol) was added dropwise. After the addition, the reaction mixture was warmed to room temperature and stirred overnight. The precipitated triethylamine salt was removed by filtration, and the filtrate was concentrated under reduced pressure. The remaining crude product was dissolved in water and extracted with dichloromethane. Evaporation of the solvent yielded an oily residue which was further purified by silica gel chromatography using methanol/chloroform (2/98, v/v) as eluent. Yellowish powder was obtained in an 82% yield. ^1H NMR (DMSO-d_6): δ 8.53 (2H, d, $J = 4.5$, 6′-py-H), 7.76 (2H, m, $J = 6.5$, 4′-py-H), 7.46 (2H, d, $J = 7.5$, 3′-py-H), 7.27 (2H, t, $J = 5.5$, 5′-py-H), 6.95 (2H, s, ph-H,), 3.87 (4H, s, py-CH_2), 3.74 (4H, s, ph-CH_2), 3.56 (4H, t, $J = 5.0$, OH−CH_2), 2.64 (4H, t, $J = 6.0$, N−CH_2), 2.23 (3H, s, ph-CH_3). ES-MS for $C_{25}H_{32}N_4O_3$: *m*/*z*, calcd ($M + H^+$) 437.25, found 437.1. Elemental analysis. Found (calcd): C, 68.56 (68.78); H, 7.21 (7.39); N, 12.83 (12.56). FT-IR spectra (ν, cm^{-1}): 3377.7 (br, s), 2917.0 (s), 2826.4 (s), 1593.3 (s), 1570.4 (m), 1478.8 (s), 1435.4 (s), 1052.3 (s), 868.9 (m), 759.5 (s).

Both intermediates of 2,6-bis(hydroxymethyl)-4-methylphenol and BCMC were prepared according to the reported procedures[20,21] with some modifications. The BCMC should be stored in a sealed bottle at −20 °C. The 2-pyridylmethyl-2-hydroxyethylamine was prepared by condensing 2-pyridine-carboxaldehyde and ethanolamine in methanol at reflux temperature and then reducing it with sodium borohydride.

Dizinc Complex (Zn_2L'). Zinc acetate dihydrate (440 mg, 1.0 mmol) dissolved in methanol was added dropwise to a stirred solution of L (218.3 mg, 0.5 mmol) in 25 mL of methanol and refluxed for 30 min in open air. After the mixture was cooled to room temperature, a white precipitate was formed 10 min later upon addition of potassium hexafluorophosphate (184.2 mg, 0.5 mmol) in portions. The precipitate was filtered and washed with methanol/diethyl ether. The yield was 475 mg (70%). Colorless block single crystals suitable for X-ray crystallographic determination were obtained by slow evaporation of the filtrate (ca. 2 weeks). The same

(27) (a) Adams, H.; Bradshaw, D.; Fenton, D. E. *Supramol. Chem.* **2001**, *13*, 513. (b) Adams, H.; Bradshaw, D.; Fenton, D. E. *Polyhedron* **2002**, *21*, 1957−1960.
(28) (a) Hough, E.; Hansen, L. K.; Birknes, B.; Jynge, K.; Hansen, S.; Hordvik, A.; Little, C.; Dodson, E.; Derewenda, Z. *Nature* **1989**, *338*, 357−360. (b) Goldberg, J.; Huang, H.; Kwon, Y.; Greengard, P.; Nairn, A. C.; Kuriyan, J. *Nature* **1995**, *376*, 745−753.
(29) Klabunde, T.; Sträter, N.; Fröhlich, R.; Witzel, H.; Krebs, B. *J. Mol. Biol.* **1996**, *259*, 737−748.
(30) Xia, J.; Shi, Y.-B.; Zhang, Y.; Miao, Q.; Tang, W.-X. *Inorg. Chem.* **2003**, *42*, 70−77.
(31) Bertini, I.; Luchinat, C.; Rosi, M.; Sgamellotti, A.; Tarantelli, F. *Inorg. Chem.* **1990**, *29*, 1460−1463.
(32) (a) Hazell, A.; Jensen, K. B.; McKenzie, C. J.; Toftlund, H. *Inorg. Chem.* **1994**, *33*, 3127−3134. (b) Chapman, W. H.; Breslow, R. *J. Am. Chem. Soc.* **1995**, *117*, 5462−5469.
(33) (a) Kaminskaia, N. V.; He, C.; Lippard, S. J. *Inorg. Chem.* **2000**, *39*, 3365−3373. (b) Vichard, C.; Kaden, T. A. *Inorg. Chim. Acta* **2002**, *337*, 173−180.
(34) Takasaki, B. K.; Chin, J. *J. Am. Chem. Soc.* **1995**, *117*, 8582−8585.
(35) Seo, J. S.; Sung, N.-D.; Hynes, R. C.; Chin, J. *Inorg. Chem.* **1996**, *35*, 7472−7473.
(36) Lambert, E.; Chabut, B.; Chardon-Noblat, S.; Deronzier, A.; Chottard, G.; Bousseksou, A.; Tuchagues, J. P.; Laugier, J.; Bardet, M.; Latour, J. M. *J. Am. Chem. Soc.* **1997**, *119*, 9424−9437.
(37) Sissi, C.; Rossi, P.; Felluga, F.; Formaggio, F.; Palumbo, M.; Tecilla, P.; Toniolo, C.; Scrimin, P. *J. Am. Chem. Soc.* **2001**, *123*, 3169−3170.
(38) (a) Koike, T.; Kajitani, S.; Nakamura, I.; Kimura, E.; Shiro, M. *J. Am. Chem. Soc.* **1995**, *117*, 1210−1219. (b) Young, M. J.; Wahnon, D.; Hynes, R. C.; Chin, J. *J. Am. Chem. Soc.* **1995**, *117*, 9441−9447. (c) Kimura, E.; Koike, T. *J. Chem. Soc., Chem. Commun.* **1998**, 1495−1500. (d) Xia, J.; Xu, Y.; Li, S.-A.; Sun, W.-Y.; Yu, K.-B.; Tang, W.-X. *Inorg. Chem.* **2001**, *40*, 2394−2401.

characteristic results were obtained for both the crystals and the powder. Elemental analysis for $C_{27}H_{39}F_6N_4O_8PZn_2$. Found (calcd): C, 39.29 (39.38); H, 4.74 (4.77); N, 6.87 (6.80). ES-MS spectra: 563.1, $[L_{-3H}Zn_2]^+$; 622.9, $[L_{-2H}Zn_2(AcO)]^+$. FT-IR spectra (ν, cm^{-1}): 1634.75 (m), 1607.06 (m), 1475.32 (m), 1440.24 (m), 842.53 (vs), 558.22 (m). ^1H NMR (DMSO-d_6): δ 8.47 (2H, s, 6′-py-H), 7.68 (2H, d, $J = 7.4$, 4′-py-H), 7.25 (2H, s, 3′-py-H), 7.11 (2H, d, $J = 7.3$, 5′-py-H), 6.41 (2H, s, ph-H), 4.37 (2H, t, $J = 10.5$, OH−CH_2), 4.04 (2H, t, $J = 10.8$, OH−CH_2), 4.18 (2H, d, $J = 16.6$, ph-CH_2), 3.77 (2H, d, $J = 7.0$, ph-CH_2), 3.96 (2H, d, $J = 26.1$, py-CH_2), 2.05 and 1.92 (2H, d, py-CH_2), 3.00 (2H, d, $J = 11.7$, N−CH_2), 2.93 (2H, d, $J = 12.4$, N−CH_2), 1.83 (Ac−CH_3, 3H), 2.43 (Ph-CH_3) overlapped with residual CH_3 of DMSO-d_6.

2.3. X-ray Crystallography. The colorless single crystal of Zn_2L' was mounted on glass fibers and used for data collection. Single X-ray diffraction data were obtained at 293 K on a Bruker Smart Apex CCD area detector using graphite monochromated Mo Kα radiation ($\lambda = 0.71073$ Å) by a 4-ω scan. The collected data were reduced using the program SAINT, and an empirical absorption correction was carried out using the SADABS program. The structure was solved by direct methods using the SHELXTL-XS program. Refinement was done with the full-matrix least-squares method on F^2 using the SHELXTL-XL program for all data with anisotropic thermal parameters for non-hydrogen atoms and isotropic parameters for hydrogen atoms.[22] Four water molecules were found to be disordered, and their occupancy was 50%.

Crystallographic data for Zn_2L' have been deposited at the Cambridge Crystallographic Data Center, CCDC No. 243433. Any inquiries relating to the data can be e-mailed to deposit@ccdc.cam.ac.uk.

2.4. Potentiometry. To determine the pK_a values of the zinc-bound water and the alcoholic hydroxyl, potentiometric pH titrations were carried out under nitrogen at 35 °C. The thermostated cell contained 20 mL of L (10.0 mM) or Zn_2L' (10.0 mM) in a water/methanol (5/1, v/v) solution with the ionic strength maintained at 0.10 M by sodium perchlorate. The titration was initiated by adding fixed volumes of 0.100 M sodium hydroxide solution in small increments to the titrated solution. Three titration experiments were performed in the pH range of 5.0−9.0. All pK_a values were reproducible to within 0.05 unit. A titration of dilute (0.0100 M) hydrochloric acid solution against sodium hydroxide with the same background electrolyte was performed to check the electrode calibration and the presence of carbonates in base solution. The pK_w (13.76 ± 0.04) was found under our conditions from the strong acid titration. A plot was made using the volume of the titrant, sodium hydroxide, versus pH. The pK_a values of the coordinated water and the alcoholic hydroxyl were obtained by sigmoidal fitting from the raw data.

2.5. Cleavage of BNPP. The cleavage of BNPP produces 4-nitrophenolate (NP) and 4-nitrophenyl phosphate (NPP). The kinetic measurements were performed by monitoring NP spectrophotometrically at 50 °C with a wavelength of maximum absorbance at 400 nm and an extinction coefficient of 18 700 L mol^{-1} cm^{-1}.[23] The substrate BNPP (50 mM in DMSO), buffers (50 mM), and varied concentrations of Zn_2L' in water/methanol (5/1, v/v) solution were prepared freshly. The reactions were initiated by injecting a small amount of BNPP into the preequilibrated buffer solutions of Zn_2L' and followed by fully mixing at 50 °C. The final concentrations of BNPP, Zn_2L', and DMSO are 0.20 mM, 0.02 mM, and 30%, respectively. In the determination of the pH-dependent cleavage reaction in an aqueous solution, pH values vary in the region of 5−9. Buffer solutions containing 20 mM *o*-phthalic acid-KOH (pH 5.0−5.5), MES-NaOH (pH 6.0−6.5), and Tris-HCl (pH 7.0−9.0) were used. The ionic strength was maintained at $I = 0.10$ M with sodium perchlorate, and the total reaction volume was 3.0 mL. After addition, the mixture was allowed to equilibrate for 5 min. Reactions were followed up to about 5% of BNPP cleavage. The pH of the solution was measured after each run, and all kinetic runs with pH variation larger than 0.1 were excluded. The absorbance values were converted into the concentration of the NP ion, and the total analytical 4-nitrophenol product was calculated using the buffer pH and the pK_a of 4-nitrophenol (2.47×10^{-7}).[24] The products of BNPP cleavage were identified by means of ^{31}P NMR and ES-MS. The pseudo-first-order rate constants, k_{obs} (s^{-1}), for the cleavage of BNPP were obtained directly from a plot of the NP concentration versus time by the method of initial rates which was linear with $R > 0.996$. In all cases, the standard deviation of the k_{obs} values was less than 6%. The second-order rate constants, k_{Zn} (M^{-1} s^{-1}), for the catalyzed reactions were determined as the slope of the linear plots of k_{obs} versus Zn_2L' concentration. All experiments were run in triplicate, and the average values were adopted. To correct for the spontaneous cleavage of BNPP, each reaction was measured against a reference cell which was identical to the sample cell in composition except for the absence of Zn_2L'.

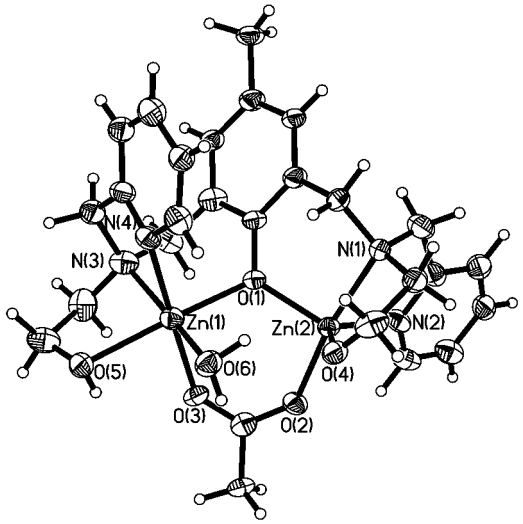

Figure 1. ORTEP drawing of the structure of the cationic core in Zn_2L'. Thermal ellipsoids for the non-hydrogen atoms are drawn at the 30% probability level. The carbon atom labelings are omitted for clarity.

The dizinc complex formed in situ from L and zinc chloride in dry DMSO was used to study the kinetics of the BNPP cleavage reaction in anhydrous medium. Zinc chloride and L were added to 3 mL of freshly distilled DMSO, and the mixture was incubated at 50 °C for 2 h to guarantee the formation of the dizinc complex (monitored by ES-MS and NMR). BNPP was injected into the mixture, and the UV−vis absorption of the solution was recorded at 400 nm after fully mixing at 50 °C. The final concentrations of BNPP and the dizinc complex were the same as those described in the aqueous system. The rate constants under these conditions were obtained by the method described above.

3. Results and Discussion

3.1. Crystallographic Structure of Zn_2L'. The structural analysis reveals that Zn_2L' crystallizes in a monoclinic *C*2/*c* space group with a molecular formula of $[Zn_2(L_{-2H})(AcO)(H_2O)](PF_6)\cdot 2H_2O$. An ellipsoid plot for the crystal structure of the cationic core in Zn_2L' with the numbering scheme is

Table 1. Summary of Crystallographic Data and Refinement Parameters for Zn_2L'

empirical formula	$C_{27}H_{39}F_6N_4O_8PZn_2$
mol wt	823.33
cryst size (mm)	0.20 × 0.26 × 0.32
temp (K)	293
cryst syst	monoclinic
space group	*C*2/*c*
a (Å)	23.935(3)
b (Å)	14.204(2)
c (Å)	22.489(3)
β (deg)	106.99(2)
vol (Å^3)	7312(2)
Z	4
μ(Mo Kα) (mm^{-1})	1.435
F(000)	3376
wavelength (Å) (Mo Kα)	0.71073
ρ_{calcd} (g/cm^3)	1.496
reflns collected	19176
unique reflns [R_{int}]	7142 [0.029]
observed data [$I > 2\sigma(I)$]	5841
θ range for data collection (deg)	1.69−26.00
GOF on F^2	1.046
final R indices [$I > 2\sigma(I)$][a]	R1 = 0.0484, wR2 = 0.1325
R indices (all data)[a]	R1 = 0.0631, wR2 = 0.1385

[a] $R1 = \sum||F_o| - |F_c||/\sum|F_o|$; $wR2 = [\sum w(F_o^2 - F_c^2)^2/\sum w(F_o^2)^2]^{1/2}$.

Table 2. Selected Bond Lengths (Å) and Angles (deg) for Zn_2L'

Zn(1)−O(1)	2.036(2)	O(1)−Zn(1)−O(3)	89.0(1)
Zn(1)−O(3)	2.156(3)	O(1)−Zn(1)−N(3)	91.9(1)
Zn(1)−O(5)	2.189(3)	N(3)−Zn(1)−N(4)	78.9(1)
Zn(1)−O(6)	2.074(3)	N(3)−Zn(1)−O(5)	78.7(1)
Zn(1)−N(3)	2.170(3)	O(1)−Zn(2)−O(2)	97.9(1)
Zn(1)−N(4)	2.155(3)	O(1)−Zn(2)−N(1)	91.1(1)
Zn(2)−O(1)	1.926(2)	N(1)−Zn(2)−O(4)	78.6(1)
Zn(2)−O(2)	1.998(3)	N(1)−Zn(2)−N(2)	79.5(1)
Zn(2)−O(4)	1.906(3)	Zn(1)−O(1)−Zn(2)	119.4(1)
Zn(2)−N(1)	2.170(3)		
Zn(2)−N(2)	2.039(3)		
Zn(1)···Zn(2)	3.421		

depicted in Figure 1. The details of the crystal data are listed in Table 1, and the selected structural parameters are given in Table 2.

The structure shows that two zinc atoms in Zn_2L' are bridged by an endogenous cresolic oxygen atom from L and an exogenous carboxyl group from acetate. The coordination number and geometry of the two zinc centers are different from each other. Zn(1) is six-coordinate and has a slightly distorted octahedral geometry. The N_2O_4 donor set is comprised of an articular tertiary amine-N, a pendant pyridyl-N, a bridging cresolic-O, a bridging carboxyl-O, an appended alcoholic-O, and an additional water-O. However, Zn(2) is five-coordinate and has a roughly trigonal-bipyramidal geometry with a donor set of N_2O_3. The bidentate bridging mode for the carboxylato unit is further confirmed by the wavenumber difference (<200 cm^{-1}) between $\nu_{asym}(COO^-)$ and $\nu_{sym}(COO^-)$ in the infrared spectra.[25] The two terminal alcoholic hydroxyls of the iminic pendant arms bind to two zinc ions at the equatorial position with a deprotonated alcohol coordinating to Zn(2) and an undeprotonated one to Zn(1). The Zn_2L' exhibits an oxygen-rich coordination environment which is crucial for biological models. Four disordered water molecules and a counterion hexafluorophosphate are also present in the structure.

The observed bond length of Zn(2)−O(4) is 1.906(3) Å, which may be the shortest length for zinc−alkoto bonds,[26] whereas that of Zn(1)−O(6) is 2.074(3) Å. The shorter bond length of the former suggests that the Zn(2)−O(4) bond is stronger than that of Zn(1)−O(6), and this may be caused by the greater electron-giving effect of O(4) toward Zn. However, the coordination status, such as the steric hindrance and coordination number of Zn(1), is different from that of Zn(2) which makes the bond length of Zn(1)−O(5) [2.189(3) Å] much larger than that of Zn(2)−O(4). Similar observations have been reported in other dizinc complexes.[27] The Zn−O distances [Zn(1)−O(3), 2.156(3); Zn(2)−O(2), 1.998(3); Zn(1)−O(1), 2.036(2); and Zn(2)−O(1), 1.926(2) Å] for the bridging acetato and cresolic groups indicate that the bridges in Zn_2L' are asymmetric. The distance between the two zinc centers is 3.421 Å, and the cresolic bridging angle [Zn(1)−O(1)−Zn(2)] is 119.36(11)°. The coordination geometries for both zinc ions observed in Zn_2L' are comparable to those found in the active sites of nuclease P1, phospholipase C, mammalian protein phosphatase-1 (PP-1), and purple acid phosphatases (PAP).[28,29] In short, complex Zn_2L' possesses the structural characteristics required for phosphoesterase mimics.

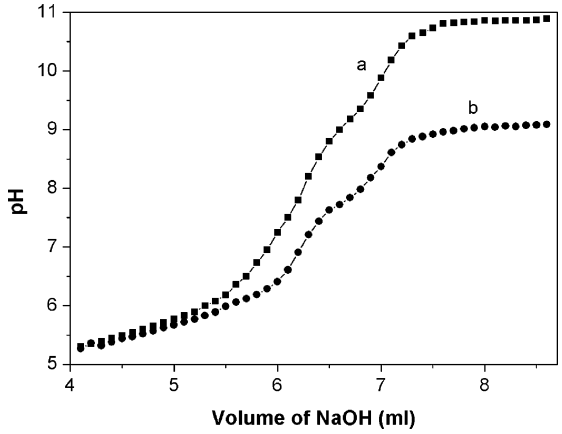

Figure 2. pH titration curves of 10.0 mM L (a) and 10.0 mM Zn_2L' in 25 mL of water/methanol (5/1, v/v) (b).

3.2. Potentiometric Studies of Zn_2L'. The potentiometric titration was carried out over a pH range of 5.0−9.0. The solution started to turn turbid when the pH was above 9 because of the precipitation of zinc hydroxide which impeded the data processing. The titration of Zn_2L' (10 mM) in water/methanol (5/1, v/v) at 35 °C and I = 0.1 M (sodium perchlorate) gave two well-defined inflections. The pK_a values were determined from the titration curve to be 7.20 and 8.15, and the deprotonating number was determined to be one at each inflection point as shown in Figure 2.

It has been found that zinc(II)−alcohol has a much lower pK_a than zinc(II)−water in the same molecule.[30] Furthermore, as mentioned above (see section 3.1), the stronger binding of the pendent alcoholic O to Zn(2) makes deprontonation of alcoholic hydroxyl easier than that of the Zn(1)-coordinated water. Therefore, the pK_{a1} of Zn_2L' can be ascribed to the deprotonation of alcoholic hydroxyl, which corresponds to the inflection point at pH 7.20. This point is comparable to that of the alcohol (pK_a 7.4) in a mononuclear zinc complex derived from an alcohol pendant macrocyclic polyamine ligand.[26a]

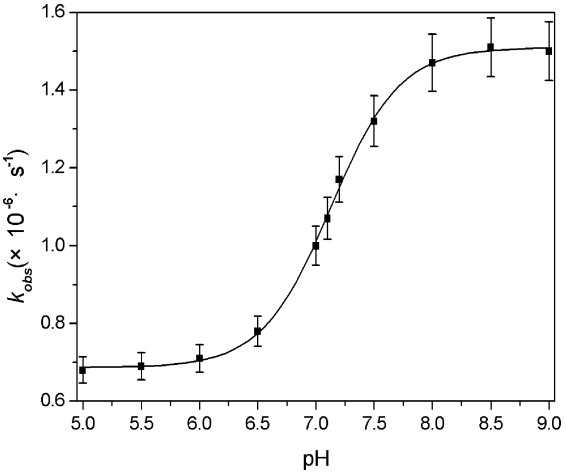

Figure 3. pH dependence of the reaction rate in an aqueous system. $[Zn_2L']_0 = 0.02$ mM, $[BNPP]_0 = 0.20$ mM, [buffers] = 50 mM, $I = 0.1$ M ($NaClO_4$), and 50 °C.

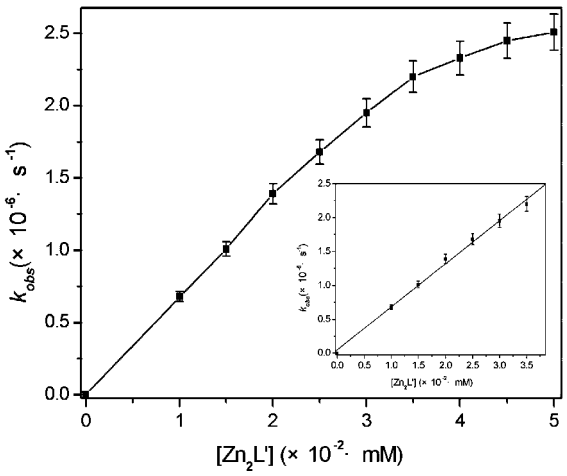

Figure 4. Dependence of the pseudo-first-order rate constant on the concentration of Zn_2L' at pH 7.20 and 50 °C. $I = 0.10$ M ($NaClO_4$), $[BNPP]_0 = 0.20$ mM, and [Tris-HCl buffer] = 50 mM.

The pK_{a2} of Zn_2L' corresponds to the deprotonation of zinc-coordinated water. Although a value of 8.15 is somewhat higher than the usual pK_a (<8) of a bridged water in dinuclear zinc(II) complexes,[9h] it is still comparable with the pK_a value of 8.0 determined for the unbridged zinc-coordinated water in an alcohol-linked triazo-macrocyclic dizinc complex.[26c] The theoretical calculations on the relationships of pK_a, coordination number, and nucleophilicity among Zn(II) complexes indicate that lower coordination numbers at the metal center lower pK_a values of bound water.[31] Thus, the relatively higher pK_{a2} value may be partly the result of the higher coordination number of Zn(1).

3.3. Phosphodiesterase Activity of Zn_2L'. BNPP is often used as a DNA model compound in the investigation of phosphodiesterase activity. The test was carried out in buffers in order to mimic biological conditions. The reaction was monitored by following the increase of absorbance at 400 nm, an indication of the release of NP from BNPP. In the determination of k_{obs}, no further release of NP from NPP was observed as evidenced by the ^{31}P NMR spectra (Figure 6).

The dependence of the reaction rate on pH for the BNPP cleavage promoted by Zn_2L' (0.02 mM) in aqueous solution at 50 °C is illustrated in Figure 3. The k_{obs} increases sharply as the pH increases from 6.5 to 8.0 and then slows at higher pHs, displaying a sigmoidal curve for the cleavage reaction. The data were fitted via a Boltzman model which resulted in a turning point at 7.13; this is near the pK_{a1} value of 7.20 obtained from the potentiometric pH titration experiments (see section 3.2). This suggests that the $-RO^-$ may be the active species responsible for the BNPP cleavage.

To determine the actual nucleophile between the alkoxide and hydroxide in the cleavage reaction, a reference experiment in absolute DMSO was performed. A second-order rate constant k_2 of 6.27×10^{-2} M^{-1} s^{-1} with respect to the dizinc complex was obtained; it is close to that in the aqueous system (vide infra). The dizinc complex was generated in situ in absolute DMSO, which was incubated with BNPP at 50 °C. After 10 h two peaks at *m*/*z* 239.1 and 784.0 were observed in the ES-MS spectra which can be ascribed to the positively charged ions of $[HNa(NPP)]^+$ and $[Zn_2LH_{-2}(NPP)]^+$, respectively. Moreover, in the negative mode of ES-MS, four negatively charged peaks with *m*/*z* values of 339.2, 174.0, 218.1, and 277.1 were observed which could be assigned to $BNPP^-$ and its cleaved products $[(NP)Cl]^-$, $[NPP]^-$, and $[H_{-1}(NP)_2]^-$, respectively (see Supporting Information). The results indicate that the dizinc complex cleaves BNPP in a water-free solution and produces the same products as those observed in aqueous media. Metal hydroxide is the commonly accepted reactive nucleophile in the phosphate-ester hydrolysis;[16b,32] however, the absence of water would suppress its formation and favor the deprotonation of alcoholic hydroxyl. Therefore, the Zn-bound deprotonated alkoxide is the nucleophile responsible for BNPP cleavage.

Figure 4 shows the effect of Zn_2L' concentrations on the k_{obs} for the cleavage of BNPP at pH 7.20 and 50 °C. The rate of BNPP cleavage initially increases linearly with the increase of Zn_2L' but gradually deviates from linearity. It is evident that the reaction is first-order for Zn_2L' only at low concentrations. The calculated pseudo-second-order rate constant for Zn_2L', k_{Zn}, determined from the plot is 6.34×10^{-2} M^{-1} s^{-1}.

The initial rate of BNPP cleavage has also been determined as a function of the substrate concentration at pH 7.20 as depicted in Figure 5. The profile reveals saturation kinetics with Michaelis−Menten-like behavior in the system, typical for native metalloenzymes. The experimental data points were fitted to the Michaelis−Menten model by evaluating from the Lineweaver−Burk double-reciprocal plot; this resulted in a Michaelis constant (K_M) of 6.15×10^{-2} M and a catalytic rate constant ($k_{cat} = V_{max}/[Zn_2L']_0$) of 4.60×10^{-6} s^{-1}. The second-order rate constant, k_{BNPP} ($=k_{cat}/K_M$), for BNPP is 7.49×10^{-5} M^{-1} s^{-1}. The reciprocal of the Michaelis−Menten constant could be treated as the substrate binding constant, that is, $K_b = 1/K_M = 16.26$ M^{-1}. The low K_b is fit for the observations that BNPP is a weak ligand for Zn_2L'.[4,33] From the kinetic data obtained under these conditions, it can be concluded that a ca. 4.2×10^5 times rate acceleration toward BNPP was obtained compared to that

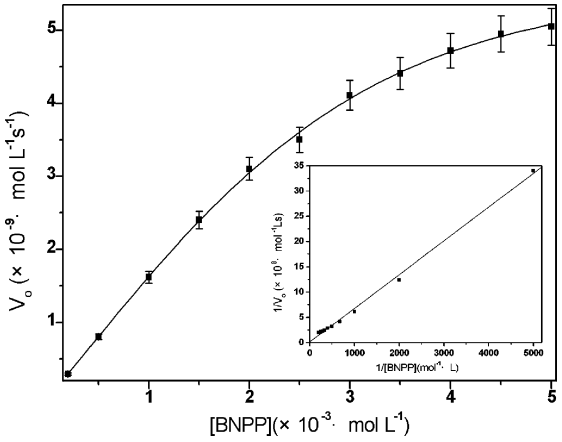

Figure 5. Saturation kinetic experiments for the cleavage of BNPP by Zn_2L' at pH 7.20 and 50 °C. $I = 0.10$ M ($NaClO_4$), $[Zn_2L]_0 = 0.02$ mM, and [Tris-HCl buffer] = 50 mM.

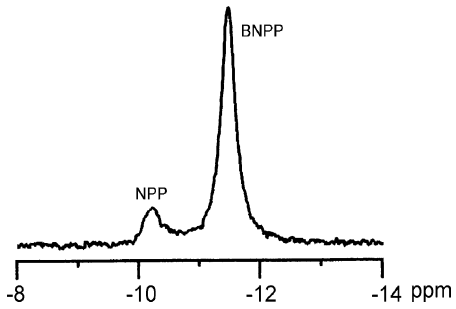

Figure 6. ^{31}P NMR spectrum recorded during the cleavage reaction of BNPP by the zinc complex of L which was generated in situ by mixing zinc acetate and L in a 2/1 molar ratio at 50 °C (BNPP is in 10-fold excess).

of the uncatalyzed hydrolysis ($k = 1.1 \times 10^{-11}$ s^{-1})[34] for Zn_2L'. These kinetic values are comparable to most other reported Zn(II)-based systems obtained under similar conditions.

The ^{31}P NMR spectroscopic method was used to further investigate the cleavage reaction at 50 °C with a solution of BNPP and the zinc complex which was formed in situ from L and zinc acetate in a molar ratio of 1/2 in DMSO-d_6 (Figure 6). The increase of the ^{31}P resonance for the cleavage product and the decrease of the ^{31}P resonance for BNPP were monitored with time. After 10 h, a notable broadening and upfield shift of about 1 ppm of the BNPP signal was observed. At the same time, a new signal attributed to the cleavage product NPP appeared at −10.3 ppm. The signal intensity ratio of the NPP to the intact BNPP is approximately 1/4. No further cleavage of NPP producing free phosphate could be detected. The observation suggests that BNPP binds primarily to the complex in the reaction via the displacement of the carboxyl bridge or the coordinated water. The ES-MS data of the reaction solution containing Zn_2L' and BNPP in methanol/water also support this conclusion. Two dominant peaks for the ions of $[Zn_2LH_{-3}]^+$ and $[Zn_2LH_{-3}(AcO)]^+$ are observed in the solution of Zn_2L' (Figure S5). After NaBNPP was added to the solution and it was allowed to stand for 10 h, two positively charged species with *m*/*z* 781.9 and 903.1 corresponding to $[Zn_2LH_{-2}(NPP)]^+$ and $[Zn_2LH_{-2}(BNPP)]^+$, respectively, formed by substitution of carboxyls were observed in the ES-MS spectra (Figure 7). The result suggests that the carboxyl and water in Zn_2L' can be exchanged and easily extruded by BNPP or NPP in the cleavage reaction.

To efficiently accelerate the process of hydrolysis, an asymmetric configuration of the metal centers is essential for the active sites of most phosphatases.[2b,3c,5] The asymmetric coordination environment and geometry for both zinc ions in Zn_2L' can meet this requirement and thus make its cleavage activity quite remarkable.

3.4. Mechanism of Phosphodiester Hydrolysis Promoted by Zn_2L'. On the basis of the kinetics data, ^{31}P NMR, and ES-MS results, a double Lewis acid activation mechanism is proposed for the Zn_2L'-catalyzed BNPP cleavage, which is similar to the reported cases.[35]

As shown in Scheme 1, the cleavage process may involve the following steps: the phosphodiester BNPP coordinates to two zinc centers as a bidentate ligand by replacing the bridging carboxyl; the zinc-bound deprotonated alcoholic

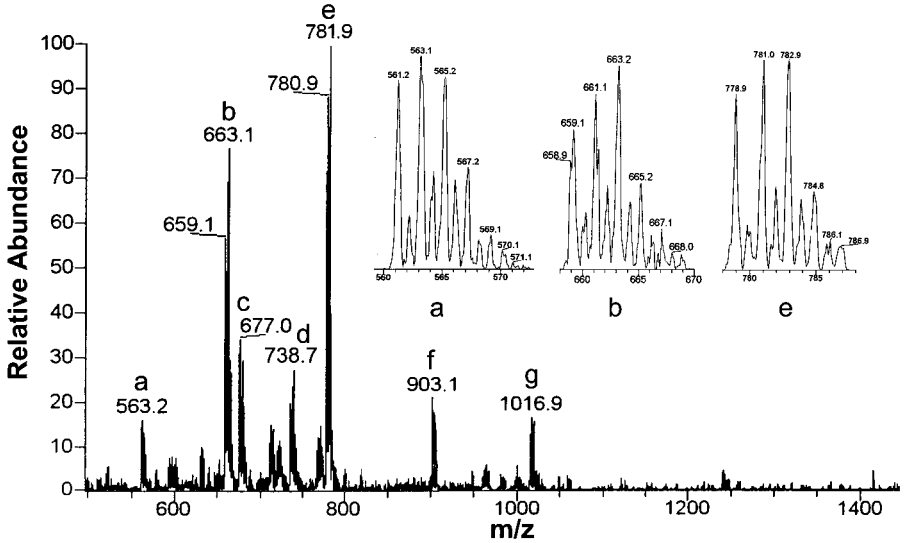

Figure 7. ES-MS spectrum of the positively charged ions for the solution of Zn_2L' and BNPP after mixing for 10 h at 50 °C in water/methanol (5/1). Detailed assignment of the detected species is listed in Table 3.

Table 3. Species Detected by ES-MS for the Solution of Zn_2L' and BNPP after Mixing for 10 h at 50 °C in Water/Methanol (5/1)

peak	species	formula	found	calcd
a	$[Zn_2LH_{-3}]^+$	$C_{25}H_{29}N_4O_3Zn_2$	561.0−570.2	564.32
b	$[NaZn_2LH_{-2}(H_2O)(AcO)]^+$	$C_{27}H_{33}N_4O_6Zn_2Na$	658.9−688.0	663.36
c	$[NaZn_2LH_{-2}(H_2O)_2(AcO)]^+$	$C_{27}H_{35}N_4O_7Zn_2Na$	675.0−684.0	681.38
d	$[NaZn_2LH_{-1}(H_2O)_2(AcO)_2]^+$	$C_{29}H_{39}N_4O_9Zn_2Na$	734.9−744.1	741.43
e	$[Zn_2LH_{-2}(NPP)]^+$	$C_{31}H_{35}N_5O_9PZn_2$	778.9−786.9	783.41
f	$[Zn_2LH_{-2}(BNPP)]^+$	$C_{37}H_{38}N_6O_{11}PZn_2$	900.8−907.8	904.31
g	$[NaZn_2LH_{-2}(H_2O)_2(AcO)(BNPP)]^+$	$C_{39}H_{43}N_6O_{15}PZn_2Na$	1014.9−1023.0	1020.00

Scheme 1. Proposed Mechanism for Zn_2L'-Catalyzed BNPP Cleavage

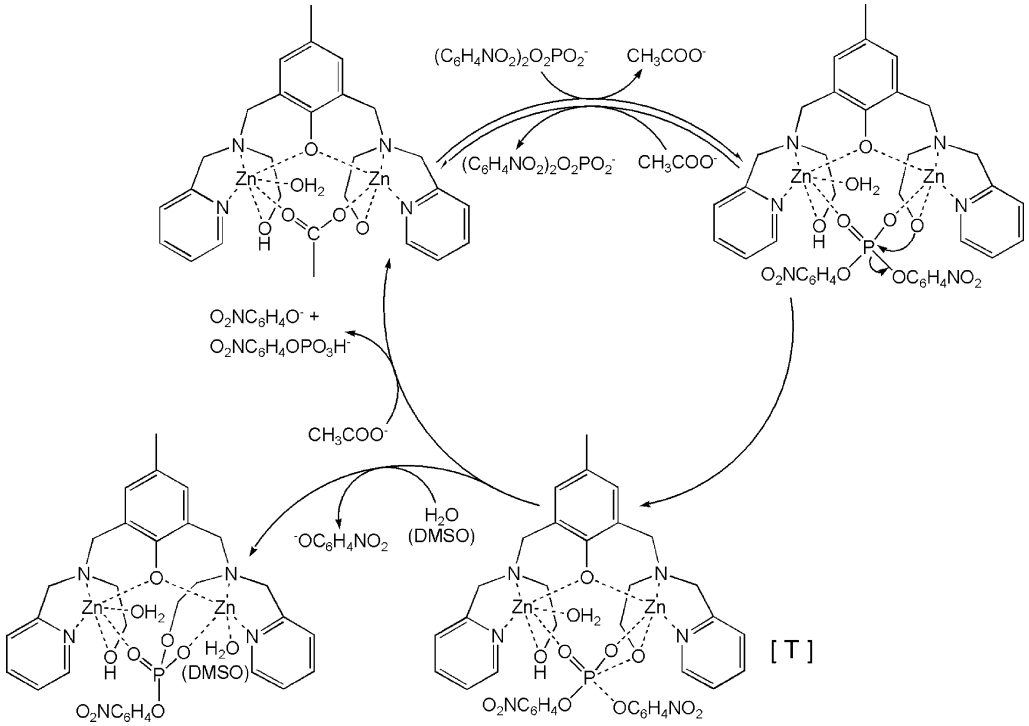

group acts as a nucleophile and attacks BNPP forming a transition complex ([T]); the P−O bond in [T] breaks to give nitrophenolate ($O_2NC_6H_4O^-$) followed by two potential processes, i.e., formation of a covalently bound Zn−NPP entity assisted by the milieu water/DMSO or reestablishment of the starting complex, Zn_2L', accomplished by the replacement of NPP with acetate. In the first step, an equilibrium may be established between Zn_2L' and the BNPP adduct because of the similar coordination potency of acetate and BNPP. The dissociation of the bridging carboxyl in Zn_2L' is quite in line with its well-documented lability.[36] The coordinated BNPP and NPP and the free cleavage products NPP and NP have been detected in ES-MS spectra as shown in Figure 7, Table 3, and Figures S9 and S10.

The intrinsic activity of dinuclear catalysts is highly dependent upon the metal−metal distance.[11b,32b,37] The appropriate intermetallic separation (3.421 Å) in Zn_2L' can facilitate the cooperative action for the phosphate bridging,[13b,d] and thus, BNPP is activated by the zinc centers as in other dinuclear metalloenzymes.[2b,4] Although the hydrolytic activity of most dinuclear complexes arises from the intramolecular attack by hydroxide coordinated to the metal ion,[16b,32] the situation for Zn_2L' is different; the deprotonated alcoholic group bound to zinc acts as the nucleophile. In fact, the functional group RO−Zn(II) in other alcoholic hydroxyl-containing complexes or some natural phosphatases was also found to be a reactive nucleophile in the hydrolysis of carboxylic esters and phosphoesterases.[6,26a,b,38]

4. Conclusion

The asymmetric dinuclear complex Zn_2L' holds essential physical features in common with the nuclease P1, phospholipase C, and the purple acid phosphatases. The complex can efficiently catalyze the cleavage of BNPP with a rate approximately 10^5-fold higher than that of the uncatalyzed reaction. The cleavage of BNPP promoted by Zn_2L' may be triggered by the phosphodiester coordination to two zinc centers in a bidentate bridging mode, followed by an attack of the deprotonated alcoholic hydroxyl to the phosphorus center, and finally leading to cleavage of the P−O bond. The correlation between the phosphatase activity and the topological architecture of a complex is an important factor to be considered in designing efficient artificial phosphatases. This research provides some insights into this issue and gives us the knowledge to obtain more efficient phosphodiesterase mimics in the future.

Acknowledgment. We thank the National Science Foundation of China (Grants 20231010, 20228102, and 30370351) for financial support.

Supporting Information Available: The ^{1}H NMR, FT-IR, and ES-MS spectra of ligand L and complex Zn_2L', the ES-MS spectra and the isotope distribution of ions for the reaction solution of Zn_2L' and BNPP, and the X-ray crystallographic file in CIF format for the structural determination of Zn_2L'. This material is available free of charge via the Internet at http://pubs.acs.org.

IC048654M